



This is a repository copy of *Strain independent twist sensor based on uneven platinum coated hollow core fiber structure*.

White Rose Research Online URL for this paper:
<http://eprints.whiterose.ac.uk/149560/>

Version: Published Version

Article:

Liu, D., Wu, Q., Han, W. et al. (9 more authors) (2019) Strain independent twist sensor based on uneven platinum coated hollow core fiber structure. *Optics Express*, 27 (14). pp. 19726-19736.

<https://doi.org/10.1364/oe.27.019726>

Reuse

Items deposited in White Rose Research Online are protected by copyright, with all rights reserved unless indicated otherwise. They may be downloaded and/or printed for private study, or other acts as permitted by national copyright laws. The publisher or other rights holders may allow further reproduction and re-use of the full text version. This is indicated by the licence information on the White Rose Research Online record for the item.

Takedown

If you consider content in White Rose Research Online to be in breach of UK law, please notify us by emailing eprints@whiterose.ac.uk including the URL of the record and the reason for the withdrawal request.



eprints@whiterose.ac.uk
<https://eprints.whiterose.ac.uk/>



Strain independent twist sensor based on uneven platinum coated hollow core fiber structure

DEJUN LIU,^{1,6} QIANG WU,^{2,7} WEI HAN,³ FANGFANG WEI,³ FENGZI LING,¹
RAHUL KUMAR,² ARUN KUMAR MALLIK,³ KE TIAN,⁴ CHANGYU SHEN,⁵
GERALD FARRELL,³ YULIYA SEMENOVA,³ AND PENGFEI WANG^{1,4,*}

¹Key Laboratory of Optoelectronic Devices and Systems of Ministry of Education and Guangdong Province, College of Physics and Optoelectronic Engineering, Shenzhen University, Shenzhen, 518060, China

²Department of Mathematics, Physics and Electrical Engineering, Northumbria University, Newcastle Upon Tyne, NE1 8ST, United Kingdom

³Photonics Research Centre, Technological University Dublin, Kevin Street, Dublin 8, Ireland

⁴Key Lab of In-fiber Integrated Optics, Ministry Education of China, Harbin Engineering University, Harbin 150001, China

⁵Institute of Optoelectronic Technology, China Jiliang University, Hangzhou, 310018, China

⁶anmeliu@163.com

⁷qiang.wu@northumbria.ac.uk

*pengfei.wang@dit.ie

Abstract: Optical fiber based twist sensors usually suffer from high cross sensitivity to strain. Here we report a strain independent twist sensor based on an uneven platinum coated hollow core fiber (HCF) structure. The sensor is fabricated by splicing a section of ~4.5-mm long HCF between two standard single mode fibers, followed by a sputter-coating of a very thin layer of platinum on both sides of the HCF surface. Experimental results demonstrate that twist angles can be measured by monitoring the strength change of transmission spectral dip. The sensor's cross sensitivity to strain is investigated before and after coating with platinum. It is found that by coating a platinum layer of ~9 nm on the HCF surface, the sensor's cross sensitivity to strain is significantly decreased with over two orders of magnitude less than that of the uncoated sensor sample. The lowest strain sensitivity of $\sim 2.32 \times 10^{-5}$ dB/ $\mu\epsilon$ has been experimentally achieved, which is to the best of our knowledge, the lowest cross sensitivity to strain reported to date for optical fiber sensors based on intensity modulation. In addition, the proposed sensor is capable of simultaneous measurement of strain and twist angle by monitoring the wavelength shift and dip strength variation of a single spectral dip. In the experiment, strain and twist angle sensitivities of 0.61 pm/ $\mu\epsilon$ and 0.10 dB/ $^\circ$ have been achieved. Moreover, the proposed sensor offers advantages of ease of fabrication, miniature size, and a good repeatability of measurement.

© 2019 Optical Society of America under the terms of the [OSA Open Access Publishing Agreement](#)

1. Introduction

Twist/torsion is a key parameter that is frequently encountered for structure health monitoring in numerous applications, such as in evaluating the health conditions of bridges, buildings, tunnels, dams and pipelines [1]. Compared to traditional electromagnetic and electronic sensors, optical fiber based twist/ torsion sensors have been attracting intensive interest due to their inherent advantages such as compact size, light weight, immunity to electromagnetic interference and a remote sensing ability.

To date, a number of optical fiber based twist sensors utilizing different fiber structures have been proposed. In general, those sensors can be mainly categorized into two types depending on their operation principles. One type is grating based twist sensors [2–8], while

the other type is based on interferometry [9–17]. Fiber grating based twist sensors suffer from relatively low twist sensitivity, complex fabrication process and expensive fabrication equipment (e.g. Excimer laser and phase masks). Interferometer based twist sensors, on the other hand, have advantages of a relatively simple fabrication process and a much higher twist sensitivity, hence a variety of fiber structure configurations based on different customized and specially designed fibers for monitoring twist have been proposed [9–17]. Among them, Mach-Zehnder interferometer (MZI) and Sagnac interferometer (SI) have been attracting most of the attention. For example, a square no-core fiber [9], a suspended twin-core fiber [10] and a tapered single mode-thin core-single mode fiber structure have been reported for twist monitoring based on MZI configurations [11]. Polarization maintaining fibers (PMFs) and photonic crystal fibers (PCFs) are widely used in SI based twist sensors [12–17]. However, most of the optical fiber based twist sensors mentioned above suffer from high cross sensitivity to strain, even for the PMFs based twist sensors which have been reported with very low cross sensitivities to temperature [14,16].

There have been a few strain insensitive twist sensors reported recently. For example, L. A. Fernandes et al. [2] reported a stress independent torsion sensor based on a helical Bragg grating waveguide structure, but the sensor itself shows a poor repeatability test of measurement. O. Frazao et al. [10] proposed a both temperature and strain independent torsion sensor based on a fiber loop mirror structure using a suspended twin-core fiber, but the sensor shows a very low twist sensitivity of $0.012 \text{ dB}/^\circ$, which may result in a large measurement error even for a small intensity variation. J. Wo et al. [5] and B. Huang et al. [13] have experimentally demonstrated strain independent high sensitivity twist/torsion sensors based on a dual-polarization distributed Bragg reflector fiber grating laser and an optical fiber reflective Lyot filter structure, respectively. However, these two sensors suffer from disadvantages of long sensor head (over 30 mm) and complex signal interrogation systems.

In our previous work, we have reported a miniature size hollow core fiber (HCF) based fiber structure with high Q transmission dips and large extinction ratios [18]. An ultra-sensitive twist sensor (up to $0.717 \text{ dB}/^\circ$) has been also demonstrated based on dip strength modulation by applying a thin layer of partial silver coating on the HCF surface [19]. However, it is found that the twist sensitivity of the HCF structure is dependent on the change of strain applied on it. To address the challenge of strain introduced variations in twist sensitivity, in this work, we propose a strain independent twist sensor based on an uneven platinum coated hollow core fiber structure. In addition, the proposed sensor is demonstrated to be able to measure strain and twist angle simultaneously by monitoring a single dip's wavelength shift and dip strength change, respectively. Usually, for optical fiber based sensors simultaneous measurement of multi-parameters is realized with multiple sensors by monitoring two or more dips' spectral responses, establishing a characteristic matrix and then the measurement result for each parameter is obtained by solving this matrix [20,21]. Compared to the complex sensor configurations and data acquisition systems used before, our proposed sensor is simpler and easier to use in real applications because only a single sensor is required to be monitored, when both strain and twist are applied to the same sensor.

2. Theoretical model and analysis

Figure 1 illustrates a schematic diagram of the proposed HCF based fiber structure with uneven platinum coating (double-sided coating as shown in Fig. 1(b)) at the outer cladding surface of HCF. Light transmission inside the fiber structure is illustrated in Fig. 1(a) only for the top half of the structure for the sake of clarity. A schematic diagram showing the cross-section of the HCF based structure after double-sided platinum coating is given in Fig. 1(b). Due to the multiple beams interferences introduced by the silica cladding, periodic transmission dips are obtained [18].

Assuming the incident light ray (L) has an amplitude A . The reflection coefficients at the interface between the inner air/cladding and cladding/ platinum /outer air are denoted as r_1 and r_2 respectively. Then the light amplitude at the end of the hollow core fiber can be expressed as follows [19]:

$$A_r = \frac{r_1 + r_2 e^{i\delta}}{1 + r_1 r_2 e^{i\delta}} A \quad (1)$$

where δ is the phase difference between the two adjacent reflected light rays inside the air core of the HCF ($L_1, L_2, L_3 \dots$) which can be calculated by

$$\delta = \frac{4\pi}{\lambda} n d \cos \theta_2 \pm \pi \quad (2)$$

where θ_2 is the refraction angle at the interface between the air core and silica cladding, d and n are thickness and refractive index of the silica cladding, λ is the incident light wavelength. The light intensity transmitted in the HCF is hence can be described as:

$$I_r = |A_r|^2 \quad (3)$$

As can be seen from the above equations, if the incident light and the physical parameters of the HCF are fixed, the transmitted light intensity is dependent on the reflection coefficients at the interfaces between the air core/cladding and cladding/platinum/outer air. r_1 and r_2 can be calculated by the Fresnel equations:

$$TE \text{ mode } r_1 = \frac{\cos \theta_1 - n \cos \theta_2}{\cos \theta_1 + n \cos \theta_2}, r_2 = -r_1 \quad (4)$$

$$TM \text{ mode } r_1 = \frac{\cos \theta_2 - n \cos \theta_1}{\cos \theta_2 + n \cos \theta_1}, r_2 = -r_1 \quad (5)$$

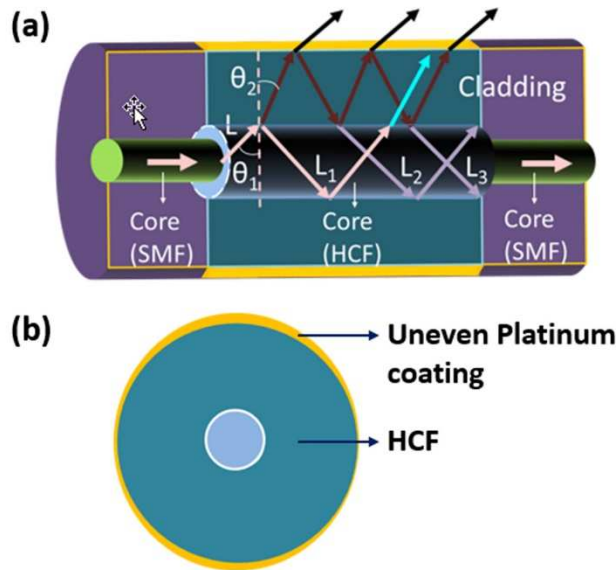


Fig. 1. (a) A schematic diagram of the proposed HCF structure, showing the light transmission and multiple beams interference inside the hollow core; (b) a schematic diagram of the HCF cross-section after coating with platinum layer.

3. Experimental setup

Here we report the experimental investigation of the influence of strain and twist on the transmission spectral of the uneven platinum-coated HCF structure. In the experiment, a short section of HCF (inner air core diameter $\sim 30\ \mu\text{m}$, outer cladding diameter $\sim 126\ \mu\text{m}$) with a length of $\sim 4.5\ \text{mm}$ was fusion spliced between two single mode fibers (SMFs). A 4.5 mm-length HCF is chosen based on our previous report, which has demonstrated that this particular HCF length produces transmission spectrum with a relatively high Q factor and low loss [17]. A sputter-coating machine (Quorum Technologies Q150RS) was used for the coating of platinum layer on the outer surface of HCF. During the coating process, the HCF fiber was fixed horizontally in the sputtering chamber and coated for a short period of time. Then the fiber sample was 180° turned over and coated for the same period of time. When the coating process is finished, a double-sided coating of platinum on the outer surface of HCF is successfully fabricated. Since the fiber surface is cylinder shaped, the coating thickness was unevenly distributed over the HCF surface, with the maximum thickness at the top/bottom of the cylinder's cross-section, decreasing towards both sides (Fig. 1(b)). In our experiment, different coating thicknesses were studied. However, it is difficult to measure the actual thickness of the platinum coating unless using a high resolution SEM because only a very thin layer of platinum (around 10 nm) was coated on the HCF surface. Therefore, the coating thickness claimed in this work is a calibrated value on a glass slide. Given that the sputter-coating machine has a platinum coating rate of $\sim 6\ \text{nm/minute}$, the coating thickness is calculated as $6\ \text{nm/minute} \times \text{Time}$. In the experiment, five fiber samples (S1 to S5) were fabricated and then coated using different time intervals of 0 seconds (s) (bare fiber sample), 30 s, 60 s, 90 s and 120 s (equivalent to calibrated coating thicknesses on a glass slide of 0 nm, $\sim 3\ \text{nm}$, $\sim 6\ \text{nm}$, $\sim 9\ \text{nm}$, and $\sim 12\ \text{nm}$), which are labeled as S1-0, S2-30, S3-60, S4-90, and S5-120, respectively.

Figure 2 shows a schematic diagram of our twist and strain sensing setup. An appropriate and fixed force was applied to different sensors to make them straight and to ensure that the same strain was applied to different fiber structure samples during the twist measurement. Twisting of the fiber structures was carried out using the fiber rotator with a twist angle resolution of circa one degree, and the axis strain was applied using the translation stage with a resolution of $10\ \mu\text{m}$. The distance between the translation stage and the fiber rotator is $\sim 20\ \text{centimeters}$. Before applying the strain/twist, the polarization state of the input light was adjusted using a manual polarization controller (PC) to achieve the largest dip strength. This initial spectrum with the largest dip strength was then labeled as a "0" twist angle state. In our experiment, a clockwise twist is defined as a negative angle twist while a counter clockwise twist is defined as a positive angle twist. Light from a broadband light source (BBS) was launched into the HCF based structure through a PC and the transmitted light was measured by an optical spectrum analyzer (OSA).

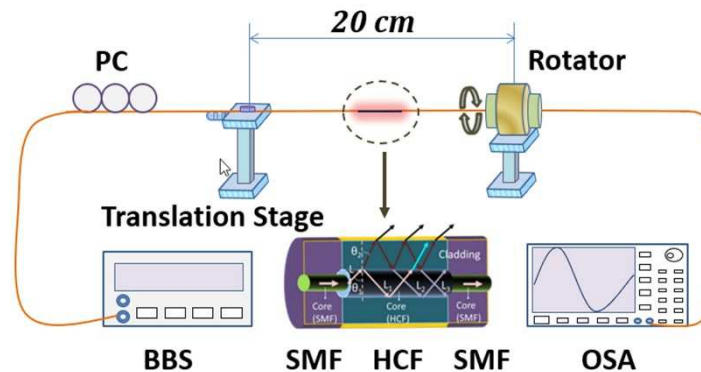


Fig. 2. Schematic diagram of the experimental setup for twist and strain measurement.

4. Results and discussion

The influence of the platinum coating thickness on the sensor's spectral response has been studied and the results are illustrated in Fig. 3, where the largest transmission dips for all the five samples (S1 to S5) are shown before and after coating with platinum by adjusting the polarization state of the input light using a PC. As can be seen from the figure, all the five bare HCF based fiber structure samples have similar transmission dips with a maximum central dip wavelengths variation of 0.25 nm and dip strengths variation of 2.18 dB, which demonstrates good reproducibility of the sensor. With the increase of the sputtering time from 30s to 120s, corresponding to an increased platinum coating thickness from ~3 nm to ~12 nm, the normalized transmission dips gradually move toward longer wavelengths, while the dip strengths show a trend of decrease. When the coating thickness is ~12 nm (S5-120), the dip strength decreased to around ~4 dB. Since the operation principle of our proposed twist sensor is based on intensity modulation, for which the twist sensitivity is highly dependent on the dip strength, hence samples from S1-0 (without coating) to S4-90 were chosen for twist experimental demonstration in the following experiment.

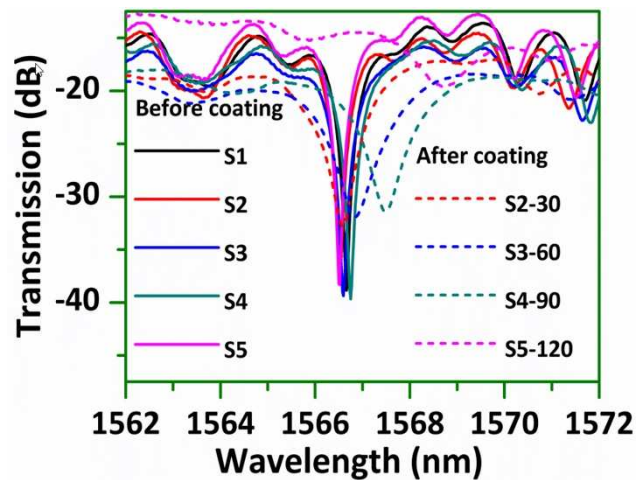


Fig. 3. Measured spectral responses of the HCF based fiber structures before and after coating with platinum layers of different thicknesses.

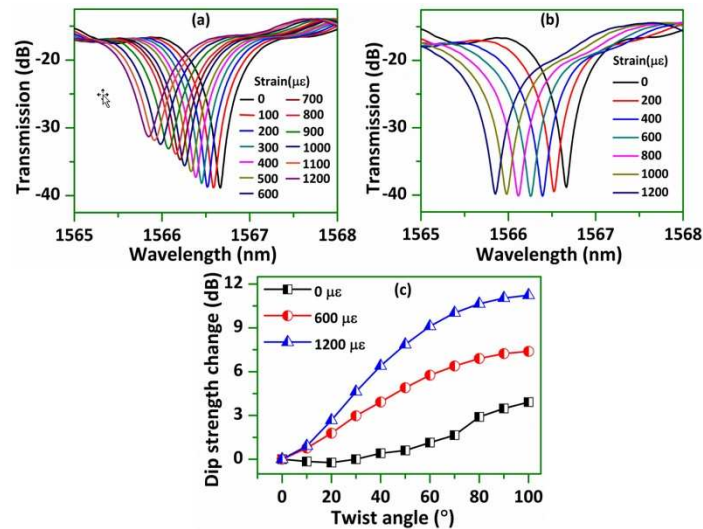


Fig. 4. Measured spectral responses of the HCF based fiber structures without platinum coating (S1-0) under different stains when the input light polarization state is (a) fixed and (b) changed; (c) Measured spectral dip strength change when twist is applied to the HCF structure at three different strain values of 0, 600 $\mu\epsilon$, and 1200 $\mu\epsilon$, respectively.

The effect of strain on the HCF sensor without platinum coating (S1-0) was firstly investigated and the experimental results are presented in Fig. 4. Before applying strain to the HCF, the transmission spectral dip was adjusted to the largest dip strength using PC. If the PC is fixed and hence the input light polarization state is maintained constant before the light enters the twist fiber section during the strain test, the spectral dip moves monotonically to a shorter wavelength with a significantly decreased dip strength (>7.5 dB) as the strain increases from 0 to 1200 $\mu\epsilon$ as shown in Fig. 4(a). However, a much smaller variation in the dip strength (<1.5 dB) is observed in Fig. 4(b) when PC is adjusted to achieve the strongest dip strength during the strain test. Ideally, a bare HCF based structure has isotropic properties, no spectral dip strength variations would be expected under strain and twist. However, this situation changes due to the existence of residual stress and core ellipticity originating from the practical fiber fabrication process, resulting in anisotropic properties and hence birefringence in the fiber structure (Birefringence is an optical property of a material in which index of refraction depends on the polarization and propagation direction of light). Birefringence induces the changes of the polarization state of the input light [22], and accordingly leads to the change of the reflection coefficients at the silica/air interface (Eqs. (4) and (5)), which eventually resulting the dip variations. It is widely reported in literature that both strain and twist produce birefringence in optical materials [22], Bigger strain applied on the HCF structure introduces larger birefringence variations and thus bigger changes in reflection coefficients at the silica/air interface, and hence a higher twist sensitivity is observed in Fig. 4(c). The average twist sensitivity measured at 1200 $\mu\epsilon$ is over three times higher than that measured at 0 $\mu\epsilon$ when the twist angle is changed from 0° to 100° . The maximum twist sensitivity at 1200 $\mu\epsilon$ is up to ~ 0.18 dB/ $^\circ$ between 10° and 40° .

Next, the effects of strain and twist on the uneven platinum coated HCF sensors were investigated. Figures 5(a) and 5(b) show the dips strength changes and their normalized dips strength change with the increase of strain for sensor samples S1-0, S2-30, S3-60, and S4-90 when the input light polarization is constant. As one can see from the figures, when the platinum coating layer thickness increases, the dip strength variation is getting smaller and smaller as the strain increases from 0 to 1200 $\mu\epsilon$. Sensor's cross sensitivity to strain is decreased by over two orders of magnitude to 2.32×10^{-5} dB/ $\mu\epsilon$ as the coating thickness

increases from 0 to ~ 9 nm, which is, to the best of our knowledge, the lowest cross sensitivity to strain for twist sensors based on intensity modulation [4,13]. It is hence concluded that in the case of the HCF structure coating with platinum helps to decrease the dependence of light polarization on the axial strain. The underlying cause of the observed strain independent properties after coating with platinum is not yet fully clear, however the decreased dip strength following coating with platinum certainly contributed to the strain independent behavior. In our previous work [19], we have theoretically demonstrated that the dip's strength decreases significantly as r_2 deviates from r_1 further (as a result of platinum layer) but with a reduced dip strength changing rate. Thus, for an uncoated HCF structure, a small variation in the reflection coefficients at the air/silica interfaces introduced by strain will produce a large dip strength change since r_2 is very close to r_1 . On the other hand, when the HCF is coated with platinum, the difference between r_2 and r_1 is increased, which leads to a much smaller dip strength change for the same reflection coefficients variations when strain is applied. Figure 5(c) shows an example of the corresponding spectral response under different strains for sample S4-90, which gives a spectral shift based strain sensitivity of 0.61 pm/ $\mu\epsilon$.

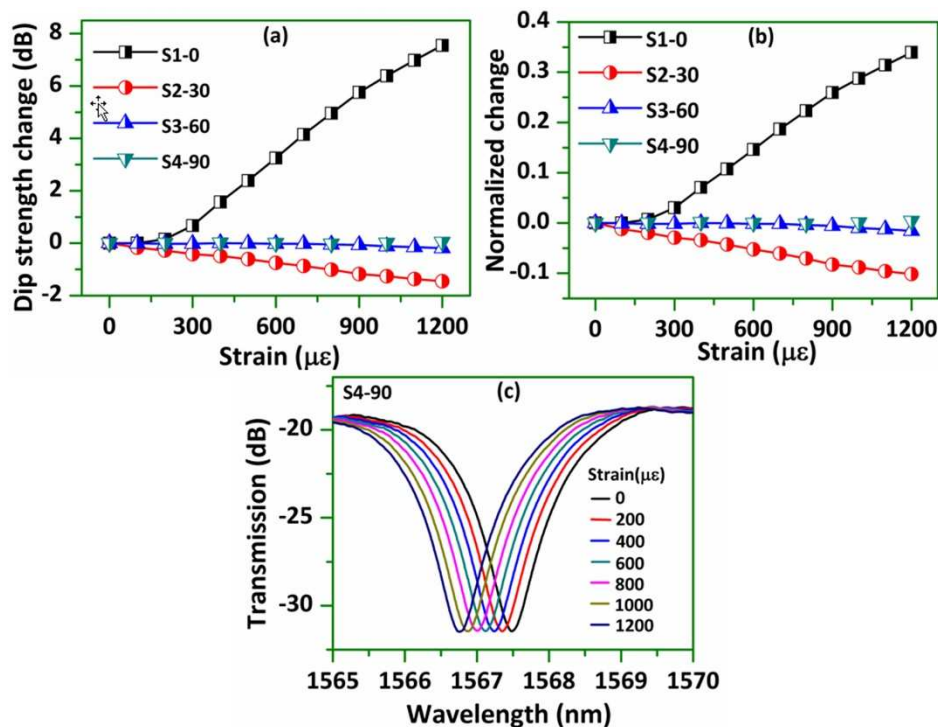


Fig. 5. (a) Measured spectral dip strength changes and (b) Normalized dip strength change when different strains are applied to sensor samples S1-0, S2-30, S3-60 and S4-90, respectively; (c) Examples of measured spectral responses of S4-90 under different strains.

Figure 6(a) shows an example of a spectral dip strength changes as the twist angle varies from 0° to 110° under applied strains of 0 $\mu\epsilon$ and 1200 $\mu\epsilon$ for sensor samples S2-30, S3-60 and S4-90. It can be seen that the measured deviation of the dip strength change is getting smaller and smaller with the increase of the platinum coating thickness, which matches well with the results shown in Fig. 5(a). Sensor S4-90 which shows the smallest dip strength change variation at 0 $\mu\epsilon$ and 1200 $\mu\epsilon$ is then chosen for a more detailed investigation of twist measurement. An example of changes in the transmission dip strength at different twist angles for S4-90 is shown in Fig. 6(b). As the twist angle increases (in both clockwise and counter-

clockwise directions), the transmission dip strength decreases monotonically while the central wavelength of the dip remains almost unchanged.

The twist sensing effect could be understood as follows. Light polarization could be described as the vector sum of S-polarized and P polarized light components. When the light incidence angle at the interface between the air core and cladding is less than the critical angle of total internal reflection, the S-polarized light is always more strongly reflected than P-polarized light [23]. Twist will introduce changes in P and S components, hence the change of reflection coefficients, and will eventually result in the dip strength change. Furthermore, a pre-designed uneven platinum coating and the actual uneven coating in all the directions introduce an asymmetric RI distribution over the outer surface of the HCF (Fig. 6(c)), leading to a large variation on the reflection coefficient at the outer silica cladding/platinum/air interface, and consequently resulting in a large power variation as illustrated in Fig. 6(b).

Figure 6(d) summarizes the changes of the spectral dip strength and their standard deviation in two rounds of increase-decrease cycles tests (four times test) as the twist angle varies from -110° to 110° . The maximum measured standard deviation is ~ 0.08 dB, which clearly demonstrates that the sensor has a very good repeatability of measurement considering the resolution of the rotator is around 1° only. The maximum twist sensitivity is ~ 0.10 dB/ $^\circ$ appears for twist angles between 20° and 40° . It is noted that the twist sensitivity is relatively low compared to our previously reported twist sensor based on a partial silver coated HCF due to a much decreased dip strength [19]. However, it is still eight times higher than a suspended twin-core fiber based twist sensor [10], six times higher than a normal FBG based twist sensor [4], three times higher than an Au-coated tilted FBG twist sensor based on surface plasmon resonance [8]. Most importantly, the proposed sensor in this work shows very low cross sensitivity to strain.

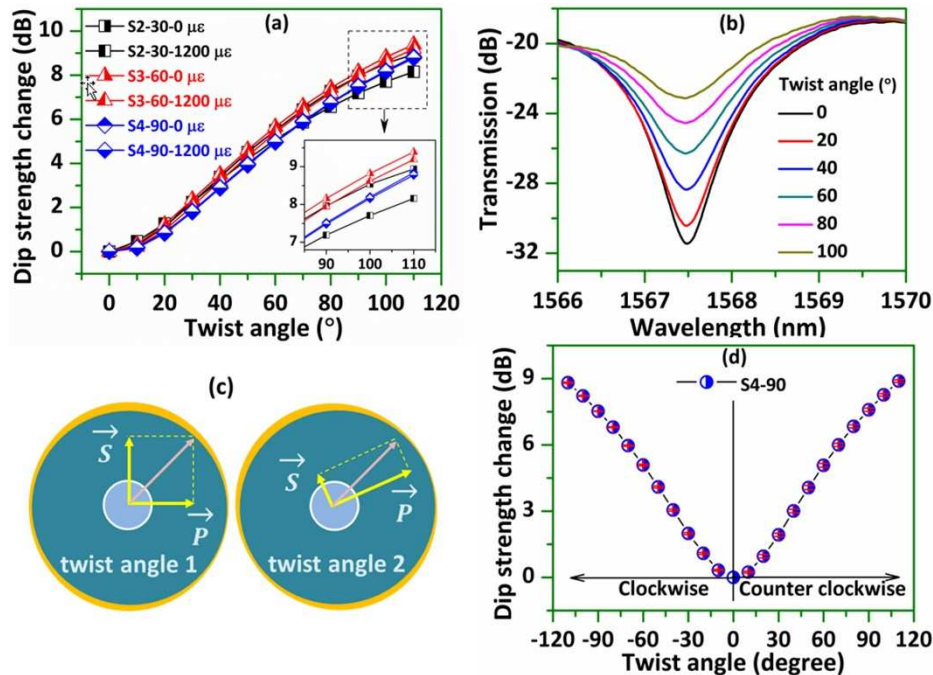


Fig. 6. (a) Measured spectral dip strength changes under twist for sensor samples S2-30, S3-60 and S4-90 at $0 \mu\text{E}$ and $1200 \mu\text{E}$, respectively; (b) An example of the measured spectral response of S4-90 under twist; (c) Schematic diagram shows the E-field orientation at different twist angles; (d) Measured spectral dip strength changes and the corresponding standard deviation in two rounds increase-decrease cycles test when twist is applied to the HCF structure.

Figures 7(a) and 7(b) illustrate standard deviation plots of the measured dip strength change under a counter clockwise twist when different strain and temperature are applied on the sensor S4-90. As can be seen from Fig. 7(a) the sensor S4-90 shows a very good performance repeatability under different strain values from $0 \mu\epsilon$ to $1200 \mu\epsilon$, with a maximum standard deviation of only $\sim 0.04 \text{ dB}$ which is even smaller than that measured in the repeatability test at $0 \mu\epsilon$, indicating that S4-90 can be used as a strain-independent twist sensor. Sensor's temperature dependence varies in the range from $22.8 \text{ }^\circ\text{C}$ to $47.4 \text{ }^\circ\text{C}$ is also investigated and shown in Fig. 7(b). The standard deviation of the measured dip strength change at different temperature values from $22.8 \text{ }^\circ\text{C}$ to $47.4 \text{ }^\circ\text{C}$, increases to $\sim 0.09 \text{ dB}$, which demonstrates that the temperature has a small effect on the dip strength and hence the twist sensitivity. Figures 7(c) and 7(d) show examples of the measured spectral dip strength variations at specific twist angles with different strains and temperatures applied. Considering a twist sensitivity of $\sim 0.10 \text{ dB}/^\circ$ for twist angles between 20° and 40° , the corresponding cross sensitivities to strain and temperature at 40° are calculated to be $\sim 9.64 \times 10^{-4} \text{ dB}/\mu\epsilon$ and $1.89 \times 10^{-2} \text{ dB}/^\circ\text{C}$, respectively. It is noted that given that the central wavelength of the dip is almost fixed during the twist test while the dip strength also does not change with the strain, it is possible to achieve simultaneous measurement of strain and twist angle by measuring the spectral shift and dip strength change, respectively.

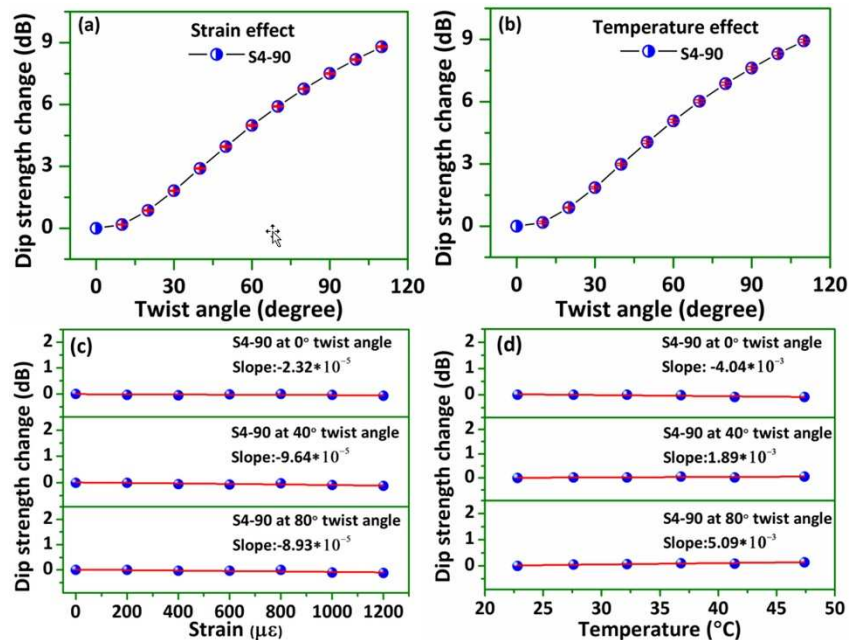


Fig. 7. Measured spectral dip strength changes and the corresponding standard deviation at (a) different axial strains applied to the HCF structure of $0 \mu\epsilon$, $200 \mu\epsilon$, $400 \mu\epsilon$, $600 \mu\epsilon$, $800 \mu\epsilon$, $1000 \mu\epsilon$ to $1200 \mu\epsilon$, and at (b) different temperatures of $22.8 \text{ }^\circ\text{C}$, $27.6 \text{ }^\circ\text{C}$, $32.2 \text{ }^\circ\text{C}$, $36.8 \text{ }^\circ\text{C}$, $41.4 \text{ }^\circ\text{C}$, and $47.4 \text{ }^\circ\text{C}$ when twist is applied to the HCF structure. Examples of measured spectral dip strength variations at specific twisted angles for (c) different strains and (d) temperatures.

5. Conclusion

In conclusion, a strain independent twist sensor is proposed and investigated based on an uneven platinum coated hollow core fiber structure. Experimental results show that strain introduces additional birefringence for the uncoated hollow core fiber structure and hence higher twist sensitivity under larger strain is observed. Sensor samples with different platinum coating thicknesses have been studied. It is found that a thin layer of platinum coating

significantly decreases the proposed twist sensor's cross sensitivity to strain. An extremely low strain sensitivity to the sensor's spectral dip strength change is demonstrated of only $2.32 \times 10^{-5} \text{ dB}/\mu\epsilon$ when the coating thickness is $\sim 9 \text{ nm}$. In addition, simultaneous measurement of strain and twist angle is achieved by monitoring the spectral dip wavelength shift and dip strength variation, with sensitivities of $0.61 \text{ pm}/\mu\epsilon$ and $0.10 \text{ dB}/^\circ$, respectively.

Funding

Shenzhen Peacock Talent Program; National Key R&D Program of China (2016YFE0126500); National Natural Science Foundation of China (61575050, 11874332); fundamental research funds for the central universities (HEUCFG201841); National major scientific research instrument development project of Natural Science Foundation of China (61727816); Department for Agriculture, Food and the Marine, Ireland (17F284).

References

1. H. N. Li, D. S. Li, and G. B. Song, "Recent applications of fiber optic sensors to health monitoring in civil engineering," *Eng. Struct.* **26**(11), 1647–1657 (2004).
2. L. A. Fernandes, J. R. Grenier, J. S. Aitchison, and P. R. Herman, "Fiber optic stress-independent helical torsion sensor," *Opt. Lett.* **40**(4), 657–660 (2015).
3. Y. J. Rao, T. Zhu, and Q. J. Mo, "Highly sensitive fiber-optic torsion sensor based on an ultra-long-period fiber grating," *Opt. Commun.* **266**(1), 187–190 (2006).
4. W. Yiping, M. Wang, and X. Huang, "In fiber Bragg grating twist sensor based on analysis of polarization dependent loss," *Opt. Express* **21**(10), 11913–11920 (2013).
5. J. Wo, M. Jiang, M. Malnou, Q. Sun, J. Zhang, P. P. Shum, and D. Liu, "Twist sensor based on axial strain insensitive distributed Bragg reflector fiber laser," *Opt. Express* **20**(3), 2844–2850 (2012).
6. L. L. Shi, T. Zhu, Y. E. Fan, K. S. Chiang, and Y. J. Rao, "Torsion sensing with a fiber ring laser incorporating a pair of rotary long-period fiber gratings," *Opt. Commun.* **284**(22), 5299–5302 (2011).
7. X. Chen, K. Zhou, L. Zhang, and I. Bennion, "In-fiber twist sensor based on a fiber Bragg grating with 81 tilted structure," *IEEE Photonics Technol. Lett.* **18**(24), 2596–2598 (2006).
8. C. Shen, Y. Zhang, W. Zhou, and J. Albert, "Au-coated tilted fiber Bragg grating twist sensor based on surface Plasmon resonance," *Appl. Phys. Lett.* **104**(7), 071106 (2014).
9. B. Song, Y. Miao, W. Lin, H. Zhang, J. Wu, and B. Liu, "Multi-mode interferometer-based twist sensor with low temperature sensitivity employing square coreless fibers," *Opt. Express* **21**(22), 26806–26811 (2013).
10. O. Frazão, R. M. Silva, J. Kobelke, and K. Schuster, "Temperature- and strain-independent torsion sensor using a fiber loop mirror based on suspended twin-core fiber," *Opt. Lett.* **35**(16), 2777–2779 (2010).
11. W. Nia, P. Lu, D. Liu, J. Zhang, and S. Jiang, "A highly sensitive twist sensor without temperature cross sensitivity based on tapered single-thin-single fiber offset structure," 25th International conference on Optical fiber sensors (OFS-25), *Proc. SPIE* **10323**, 103235D (2017).
12. B. Song, H. Zhang, Y. Miao, W. Lin, J. Wu, H. Liu, D. Yan, and B. Liu, "Highly sensitive twist sensor employing Sagnac interferometer based on PM-elliptical core fibers," *Opt. Express* **23**(12), 15372–15379 (2015).
13. B. Huang, X. Shu, and Y. Du, "Intensity modulated torsion sensor based on optical fiber reflective Lyot filter," *Opt. Express* **25**(5), 5081–5090 (2017).
14. H. M. Kim, T. H. Kim, B. K. Kim, and Y. J. Chung, "Temperature-insensitive torsion sensor with enhanced sensitivity by use of a highly birefringent photonic crystal fiber," *IEEE Photonics Technol. Lett.* **22**(20), 1539–1541 (2010).
15. T. Hu, Y. Zhao, and D. Wu, "Novel torsion sensor using a polarization maintaining photonic crystal fiber loop mirror," *Instrum. Sci. Technol.* **44**(1), 46–53 (2016).
16. P. Zu, C. C. Chan, Y. X. Jin, T. X. Gong, Y. F. Zhang, L. H. Chen, and X. Y. Dong, "A temperature-insensitive twist sensor by using low-birefringence photonic-crystal-fiber-based Sagnac interferometer," *IEEE Photonics Technol. Lett.* **23**(13), 920–922 (2011).
17. W. Chen, S. Lou, L. Wang, H. Zou, W. Lu, and S. Jian, "Highly sensitive torsion sensor based on Sagnac interferometer using side-leakage photonic crystal fiber," *IEEE Photonics Technol. Lett.* **23**(21), 1639–1641 (2011).
18. D. Liu, Q. Wu, C. Mei, J. Yuan, X. Xin, A. K. Mallik, F. Wei, W. Han, R. Kumar, C. Yu, S. Wan, X. He, B. Liu, G.-D. Peng, Y. Semenova, and G. Farrell, "Hollow Core Fiber Based Interferometer for High Temperature (1000 °C) Measurement," *J. Lightwave Technol.* **36**(9), 1583–1590 (2018).
19. D. Liu, R. Kumar, F. Wei, W. Han, A. K. Mallik, J. Yuan, C. Yu, Z. Kang, F. Li, Z. Liu, H.-Y. Tam, G. Farrell, Y. Semenova, and Q. Wu, "Highly sensitive twist sensor based on partially silver coated hollow core fiber structure," *J. Lightwave Technol.* **36**(17), 3672–3677 (2018).

20. D. Liu, R. Kumar, F. Wei, W. Han, A. K. Mallik, J. Yuan, S. Wan, X. He, Z. Kang, F. Li, C. Yu, G. Farrell, Y. Semenova, and Q. Wu, "High sensitivity optical fiber sensors for simultaneous measurement of methanol and ethanol," *Sens. Actuators B Chem.* **271**, 1–8 (2018).
21. H. Lu, Y. Yue, J. Du, L. Shao, T. Wu, J. Pan, and J. Hu, "Temperature and liquid refractive index sensor using P-D fiber structure-based Sagnac loop," *Opt. Express* **26**(15), 18920–18927 (2018).
22. V. Budinski and D. Donlagic, "Fiber-optic sensors for measurements of torsion, twist and rotation: a review," *Sensors (Basel)* **17**(3), 443 (2017).
23. C. A. Dimarzio, *Optics for Engineers* (CRC, 2011), pp. 147.